

Charged Particle Microscopy: Why Mass Matters

John A. Notte

Carl Zeiss NTS, LLC, One Corporation Way, Peabody, MA 01960

john.notte@zeiss.com

Introduction

From the nearly mass-less electron to massive ions, charged particle microscopes have diversified over the last few decades. At present, a broad range of available charged particles with varying masses fulfill many applications: from imaging to analysis to nanofabrication.

Charged particle microscopes play a valuable role for applications that require high-resolution images and small focused probe sizes—well beyond what can be achieved with traditional light microscopes. The scanning electron microscope (SEM) and the gallium focused ion beam (Ga-FIB) represent the low-mass and high-mass range of the commonly available commercial instruments. These two beams often work collaboratively on a single instrument—each offering strengths not afforded by the other. In the past several years, the gas field ion source (GFIS) technology has enabled the usage of helium ions [1], which are much more massive than the electrons but still lighter than most elements on the periodic table. The same GFIS technology may also provide a focused neon beam, which may enable capabilities not afforded by the other charged particle beams [2]. The unique role of each of these four charged particle beams (e⁻, He⁺, Ne⁺, Ga⁺) is determined almost entirely by their mass. This article offers a survey of these four charged particle beams, with particular consideration given to the physics of focused probe formation and sample interaction and how this depends critically on each particle's mass. Finally, the different sample interactions are compared for applications of imaging, analysis, and nanofabrication.

Historical Background

The first microscopes were based on biomimicry: In the 1670s Leeuwenhoek assembled optical lenses to aid our otherwise unaided eye in visualizing the smallest details. Such light optical microscopy was simple to interpret because our brains and eyes had accumulated three million years of experience with the interpretation of such images and the contrast mechanisms they provide. In the three centuries since, light microscopy has flourished with many variations and specializations of this technology. However at the highest magnifications, light microscopy meets its limitations. The wave-like nature of light means that it will suffer from diffraction effects upon passing through an aperture—an essential component of microscopes to control aberrations. This effectively restricts photons to imaging applications where the features of interest are larger than, or comparable to, the wavelength of light.

In the last half century, to supplement the photon, we have called upon its massive counterparts, the electron and the much more weighty ions, to reveal smaller features. The family of charged particles microscopes (CPM) is now diverse and multifunctional. Their advantage versus the photon arises from their having an appreciably smaller

wavelength compared to typical photons. They can provide imaging at remarkable resolution, even sufficient to resolve adjacent atoms. The CPM images provide their own contrast mechanisms that reveal topographic, compositional, or electrical properties and convert these pieces of information into images that can easily be interpreted. Some charged particle beams excel at providing analysis—providing unambiguous elemental information about the sample in question. In some cases, charged particle beams serve as hands as well as eyes, giving us the ability to manipulate matter at the nanoscale as well as see it.

Probe Formation: Why Mass Matters

Within the charged particle microscope, the mass of the particle determines the technology best suited to accelerate, deflect, and focus a beam of particles. A particle of charge, q , which is accelerated through a potential difference, V , gains a kinetic energy, qV . However, the corresponding velocity varies drastically with mass, as shown in Table 1.

It is important to note that at 20 keV, the electron's speed is comparable to the speed of the electrons whizzing about within the inner shells of the heavier atoms; indeed it is one-fourth the speed of light! The speed of the charged particle has tremendous importance in its interaction with matter, a factor that is critical for analysis, which we will consider later. It is also interesting to consider a 100 pA beam current, which corresponds to 6×10^8 particles striking the sample every second (a rate that is independent of mass). Under these conditions, the typical spacing between successive high-energy electrons would be 130 nm (there may be only one between the aperture and the sample), whereas the successive gallium ions are crowded to within half a millimeter of each other.

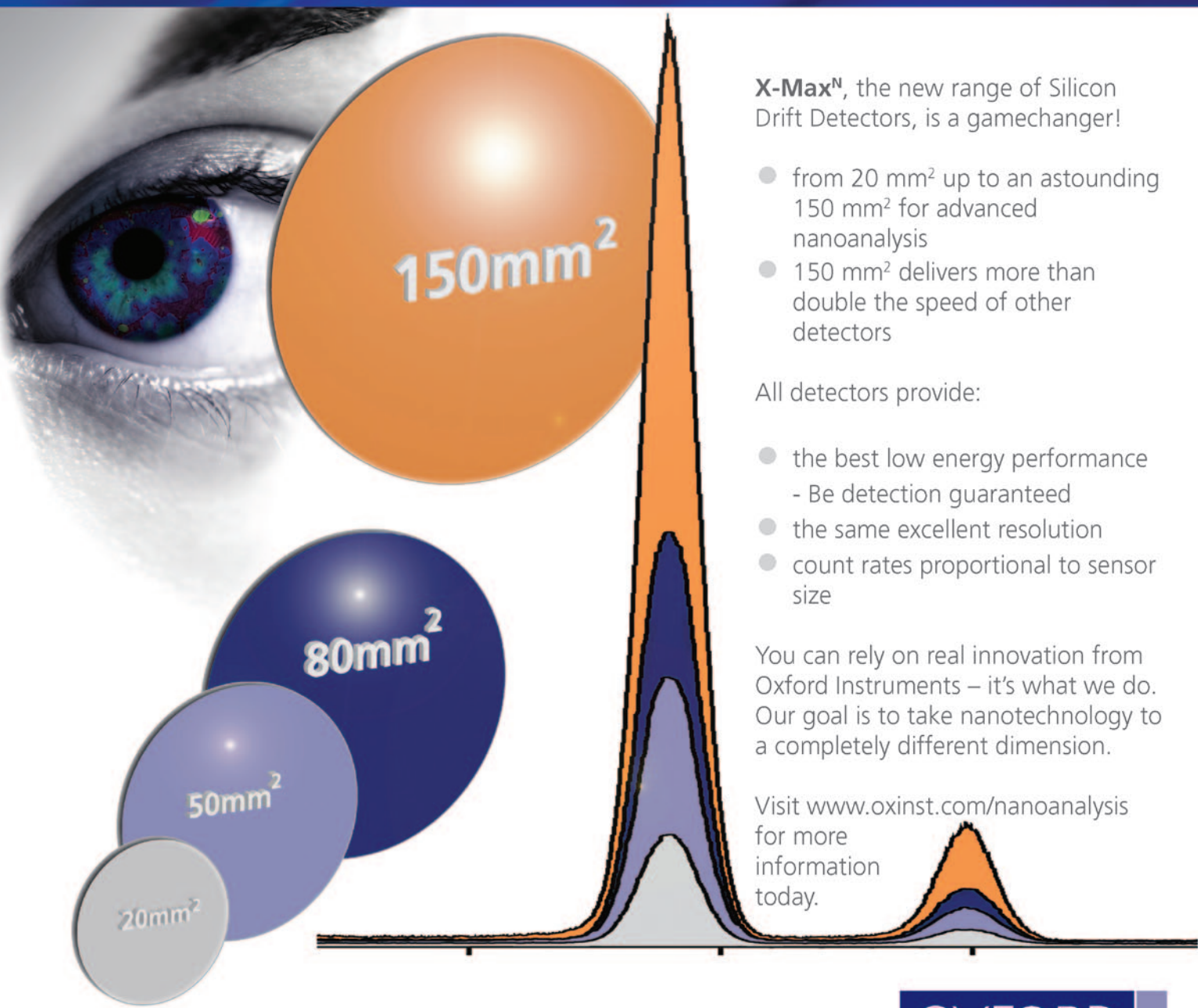
The forces available for the steering and focusing of charged particles are derived from electric fields, E , and

Table 1: The velocity of the charged particles that are commonly used in charged particle microscopy. The electron's data is presented at two energies because it is commonly used in the SEM at low energies for imaging and at higher energies for analysis. The atomic mass unit, amu = 1.66×10^{-27} kg.

Charged Particle	Mass (amu)	Velocity after Acceleration (m/s)
Electron	5.5×10^{-4}	1.9×10^7 (with 1 keV energy)
		8.4×10^7 (with 20 keV energy)
Helium	4.00	1.20×10^6 (with 30 keV energy)
Neon	20.2	5.35×10^5 (with 30 keV energy)
Gallium	69.7	2.88×10^5 (with 30 keV energy)

Introducing X-Max^N – SDD for Nanoanalysis

Size matters, sensitivity counts



X-Max^N, the new range of Silicon Drift Detectors, is a gamechanger!

- from 20 mm² up to an astounding 150 mm² for advanced nanoanalysis
- 150 mm² delivers more than double the speed of other detectors

All detectors provide:

- the best low energy performance - Be detection guaranteed
- the same excellent resolution
- count rates proportional to sensor size

You can rely on real innovation from Oxford Instruments – it's what we do. Our goal is to take nanotechnology to a completely different dimension.

Visit www.oxinst.com/nanoanalysis for more information today.

www.oxford-instruments.com



The Business of Science®



magnetic fields, B . The Lorentz force law describes the acceleration, a , of a particle of mass, m , and charge, q :

$$\vec{a} = \frac{q}{m} (\vec{E} + \vec{v} \times \vec{B}) \quad (1)$$

A particle passing through a region of length, L , of transverse electric or magnetic field will be deflected by a small angle, θ , from its original trajectory:

$$\theta = \frac{EL}{2V} \quad (\text{electrostatic}) \quad (2)$$

$$\theta = BL \sqrt{\frac{q}{2mV}} \quad (\text{magnetostatic}) \quad (3)$$

Note that the electric field deflection is independent of both the charge and the mass of the particle. The interesting consequence is that doubly charged ions, or even different mass isotopes will follow the same trajectory in purely electric fields—provided that they were accelerated by the same potential, V . However, for magnetic fields, the mass dependence now arises, as does the charge dependence. This is the basis for mass and charge separation by use of magnetic fields. For the electron, it is possible to use either electric or magnetic fields to deflect these particles, whereas for the more massive ions, the same magnetic field will only produce relatively weak deflections. Thus, commercial ion microscopes use electrostatic elements for deflection, focusing, and stigmation, whereas electron beam systems can use any combination of magnetic and electric fields for these same purposes.

Quantum mechanics taught us that the distinction between particles and waves is not so clear-cut: photons have momentum, whereas particles can exhibit wave-like properties. Therefore the same diffraction effects that limit the utility of light microscopes can also impact charged particle microscopes. The deBroglie wavelength for each of these particles (at their typically used beam energy) is shown in Table 2. The same table also includes their contribution to the final focused probe size [3] under their typical beam convergence angle, α .

At this point it is evident that the typical low-voltage SEM will be impacted by diffraction effects, as well as chromatic aberration, when attempting to produce images at the nanometer scale. There are various ways to attempt to

circumvent the diffraction effects of electron beams. One strategy is to use larger convergence angles, which requires the introduction of aberration-corrected optics. This leads to system complexity and other compromises such as depth of field. An alternate strategy is to use higher energy electron beams. While this decreases the chromatic and diffraction effects, it causes the electron beam to penetrate more deeply, requiring the usage of metal coated samples, or samples with a relatively uniform subsurface, or even pre-thinned samples for the TEM. In contrast, diffraction does not significantly degrade the focused probe size for most ion beams. This is not to say that the electrons are less valuable because of their low mass; their low mass gives them great virtues that will be evident shortly.

Sample Interaction: Why Mass Matters

As the beam impinges upon the sample, the individual charged particles undergo a series of collisions with the atomic electrons and nuclei that comprise the sample. Here too, the mass of the incident particle plays a defining role in the nature of this scattering and its usefulness in various applications. The random nature of the scattering allows the use of simulation software [4, 5] to better understand and visualize the typical scattering effects. Figure 1 shows the results of these simulations.

Incident electrons are scattered elastically by atomic nuclei in the atoms encountered along their trajectory in the sample. The mass inequity causes the electron to suffer a significant angular deflection—often backscattering out of the sample. The backscattering probability increases with atomic number up to 50 percent, an effect that provides compositional imaging in the SEM. Incident electrons also can interact inelastically with the electrons in the atoms of the sample, scattering into small angles and losing significant amounts of energy by various means. As a consequence of these scattering processes, the once collimated incident beam broadens beneath the surface into an interaction volume that increases in size with beam energy [6].

Incident ions, because of their larger mass, scatter primarily from nuclei of sample atoms. Ions interact only weakly with the electrons of the sample, producing small angular deflections and very limited energy losses. Thus, it is the scattering from the nuclei that most greatly impacts the trajectory of the incident ions. For lower mass ions (for example, helium) these nuclear scattering events will dominate only when the incident ion has lost most of its energy and is moving at a slower velocity. Hence the focused helium beam stays relatively collimated as it penetrates into the sample. Eventually enough energy is lost and nuclear scattering dominates, leading the abrupt “tangles” at the end of their trajectories (evident in Figure 1). For heavier ions with larger atomic numbers (neon and gallium), the nuclear scattering plays a role immediately upon penetration. Nuclear

Table 2: The various charged particles with their deBroglie wavelength are shown. Also shown is the contribution of diffraction in determining their final focused probe size.

Charged Particle	Mass (amu)	deBroglie Wavelength (pm)	Diffraction Contribution to Probe Size (nm)
Electron	5.5×10^{-4}	38.8 (at 1 keV)	2.1 (at $\alpha = 10$ mrad)
		7.08 (at 20 keV)	0.47 (at $\alpha = 10$ mrad)
Helium	4.00	0.083 (at 30 keV)	0.149 (at $\alpha = 0.3$ mrad)
Neon	20.2	0.037 (at 30 keV)	0.066 (at $\alpha = 0.3$ mrad)
Gallium	69.7	0.020 (at 30 keV)	0.001 (at $\alpha = 10$ mrad)

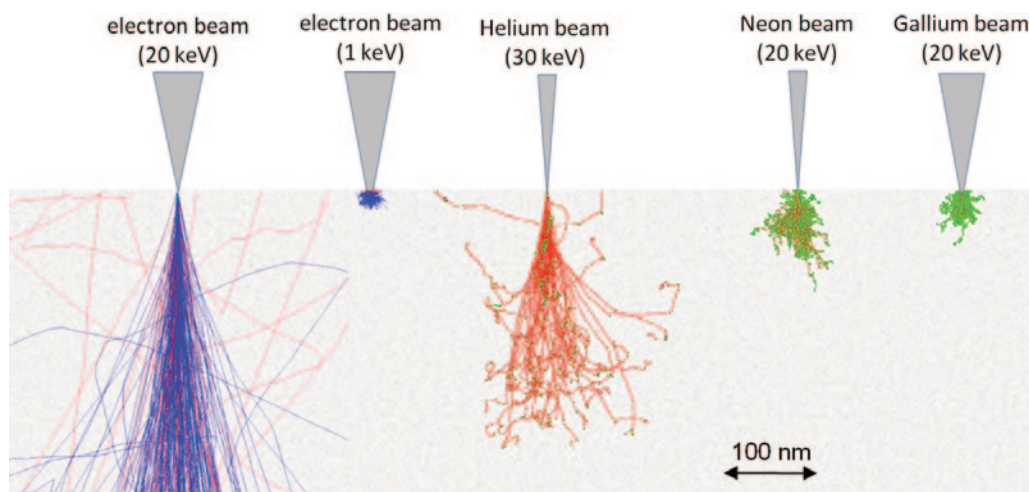


Figure 1: Simulations for 20 keV and 1 keV electron beams, a 30 keV helium beam, and 20 keV neon and gallium beams. The electron trajectories are shown in blue, and backscattered electrons are shown in red. The ion trajectories are shown in red, and the trajectories of recoiled sample atoms are shown in green. The simulated sample here is aluminum.

scattering leads to the displacement of the target nuclei (shown in green in Figure 1) from their original locations, including surface sputtering of atoms. Although backscattering is always possible, it is much less likely when the incident particle is heavier than the scattering targets. For example, $M_{\text{He}} < M_{\text{Al}} < M_{\text{Ga}}$, so helium will backscatter from aluminum (about 1 percent of the time), but the backscatter yield of gallium ions on aluminum is much, much lower (see Table 3).

Through all of these collisions, the incident particle will eventually expend all of its energy and come to rest. It will be implanted at some depth into the material, inducing stress in the lattice and perhaps other changes to the specimen. In some semiconductor applications, the electrical, chemical, and optical effects of gallium can be quite negative, so the neon beam offers much needed relief. In other applications, these effects are quite negligible and can be tolerated [7] or even exploited [8]. For typical SEM energies, the electrons possess much less momentum than ions and produce almost no lasting effects as they strike the sample. The only exception is in the case of highly insulating samples where the implanted electrons can cause sub-surface charging that can accumulate and cause damage.

Imaging: Why Mass Matters

Scanning charged particle microscopes generate their images by rastering the focused beam across the sample and assigning a gray level to each pixel of the image according

to the intensity of some detectable signal. Secondary electrons (SEs) are produced in great abundance, and they convey valuable information such as topographical. It is quite remarkable that these SEM images are so intuitively interpreted by our brains that have evolved for millions of years to interpret light images. Secondary electrons typically have energies of 10 eV or less and are produced all along the trajectory of the incident charged particle. Their probability of escape from the sample and subsequent detection depends critically on their distance from the surface with

a typical escape depth limited to just a few nanometers [9]. Hence for the best imaging resolution, the charged particle beam should diverge slowly as it penetrates into the sample so that SEs are emitted primarily from under the footprint of the incident beam. These secondary electrons can be produced at several locations: (a) where the incident beam first enters the sample, (b) where backscattered particles exit the sample, and (c) where sputtered atoms exit the sample. If (a) were the dominant mechanism for all beams, then the image resolution would be determined solely by the focused probe size and its sub-surface divergence. However, for the low-voltage SEM, a significant fraction of the SEs originate from mechanism (b), somewhat degrading the image resolution it can offer. For neon and gallium ions, there is a wholesale excitation of the sample very close to the surface that produces significant SEs at locations (a), (b), and (c). The higher sputtering yields of neon and gallium beams also limit the attainable image resolution simply because the sample is dynamically changing during the imaging process [10]. Note again that their high sputter rate is a consequence of their mass. Here, the helium ion's intermediate mass is responsible for an important imaging advantage: the beam diverges slowly within the sample, and the sputter yield and backscatter yield are low enough to minimize the SEs produced in the surrounding region. Thus, most SEs originate from location (a). This conclusion is not universal for all samples, especially when implantation of helium must be avoided.

Table 3: Comparing the incident ions' interactions in aluminum and gold samples. Data derived from the SRIM [5] simulation of 10,000 incident ions at normal incidence.

Incident Beam	Aluminum Sample			Gold Sample		
	Backscatter Yield	Vacancies per Ion	Sputter Yield	Backscatter Yield	Vacancies per Ion	Sputter Yield
30 keV He	0.0093	81	0.06	0.188	80	0.153
30 keV Ne	0.0075	375	1.78	0.279	508	4.39
30 keV Ga	<0.0001	487	3.90	0.134	722	17.4

Analysis: Why Mass Matters

A good microscopist will spend only a moment appreciating a good image before he starts asking the next question: what is the sample made of? Thus, it would be useful to obtain a compositional analysis with the very same charged particle microscope. At its most basic, analysis refers to elemental composition, but it could also include chemical bond information, crystallographic information, depth distributions, and so on. For the four charged particles under consideration, the mass is the primary factor in determining the analytical strategies and strengths for each.

Both X-ray and Auger electron spectrometries rely on the initial excitation of inner shell electrons of the atoms comprising the sample [11]. The ability of the incident particle to efficiently excite inner shell electrons is based on a velocity matching criteria [12]. Given that most commercial instruments operate at 30 keV and below (for stability, safety, and cost reasons), this velocity matching condition is determined mostly by the mass of charged particle. For an electron accelerated to 20 keV, its velocity roughly matches the velocity of the inner shell electrons of many atoms. Hence, electron beams are remarkably effective at inducing X-ray emission. Today there is a variety of silicon drift detectors (SDD) and supporting software that can measure and identify characteristic X rays with high reliability and high speed. Elemental “maps” can now augment the traditional SE image. An example of such a map with specific elements encoded by color is shown in Figure 2. These maps are necessarily of lower spatial resolution (both lateral resolution and depth resolution) because X rays can escape from anywhere within the excited volume. In contrast, the helium, neon, and gallium ion beams are virtually useless for production of X rays because of their higher mass and, hence, lower velocity.

Although not suitable for X-ray production, 30 keV ion beams still offer some valuable analytical capabilities. The small fraction of ions that backscatter out of the sample convey information about the depth of the scattering event combined with information about the mass of the scattering nucleus.

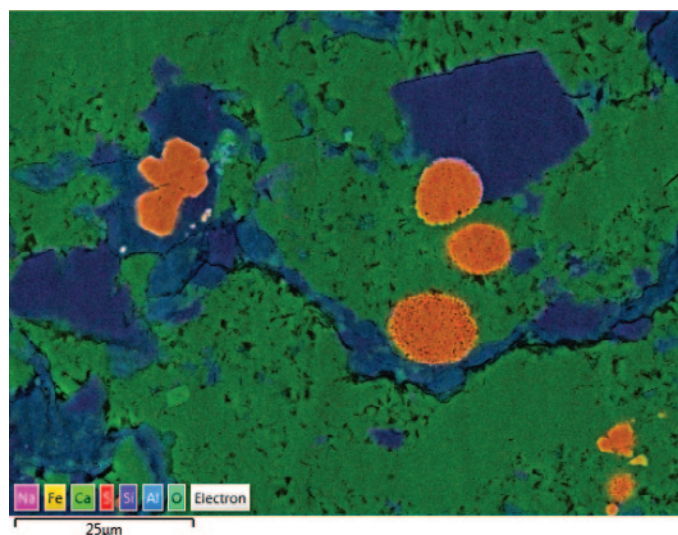


Figure 2: Elemental map generated with a 30 keV electron beam. Image provided by Jeff Marshman.

Such ion scattering analysis is already established [13] and commercially available [14], but the information it produces is not as simply interpreted as the characteristic X rays that electrons can generate. As another option, the ion beams that are massive enough to sputter efficiently (specifically the neon and gallium beams) can be coupled with secondary ion mass spectrometers (SIMS). There are a variety of SIMS detectors including magnetic quadrupoles and time-of-flight systems that reveal the mass of the sputtered atoms or molecules [15].

Nanofabrication: Why Mass Matters

The ability to see and to analyze at the nanometer scale invites the eager researcher to manipulate matter at this same fine scale. Such nanofabrication with charged particle beams can be achieved by a variety of means, such as direct-write lithography, gas-assisted beam chemistry (deposition and etching), and patterned sputtering. For each of these, the relative performance of these four charged particle beams is, again, a simple consequence of their mass.

For lithography, the electron beam has been effectively used to pattern features as small as 10 nm in resists such as HSQ and PMMA [16]. More recently, helium [17] and neon [18] ion beams have also produced sub 10 nm features in HSQ. The advantages of helium and neon arise from their intermediate masses; they remain relatively collimated within the sample (Figure 2) and therefore reduce the proximity effects, that is, unintended exposure outside the scanned pattern, that complicate electron beam lithography. For beam-induced chemical processes (both etching and deposition) good results have been obtained by all of these four charged particle beams. Although the mechanisms are not fully understood, the features produced are measured in the tens of nanometers—seemingly limited by factors other than focused probe size. In some cases, the electron beam is at a disadvantage because its low mass cannot sputter away oxides or reaction products. In the case of insulator deposition, the gallium beam can leave residual metal atoms that limit its resistivity. Work in this area with helium and neon is still at the very early stages.

For sputtering applications, the electron beam falls far behind the ion beams. The gallium beam excels at the removal of large amounts of material. Its first advantage is its large mass and hence the large sputter yield (Table 3). Second, the LMIS technology can produce beam currents as large as 100 nA—at least 3 orders of magnitude more than can be produced with the GFIS technology. Thus gallium is better suited for removing cubic *microns* of material. However, gallium will leave residual metal ions that can adversely affect final properties. Also, the larger interaction volume of gallium makes it less well suited for the milling of very fine details. For the finer details, the focused neon ion beam offers more precision, albeit at a lower sputter yield. For the finest details, the helium ion beam offers a sub-nanometer probe size and a sputter rate that is suited for such fine work as the milling of graphene [19]. It should be noted that the sputtered atoms arise from a multi-step process that causes the sputtered region to be somewhat larger than the focused probe [20].

Because the sputter rate trend (Ga > Ne > He) is opposite to the precision trend (He > Ne > Ga), these three ion beams are

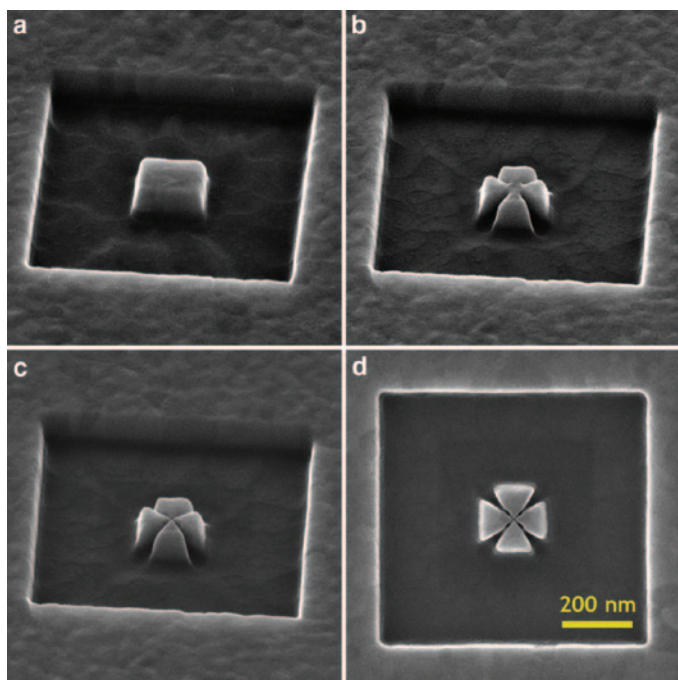


Figure 3: The bulk milling of the gold on glass substrate is achieved with the gallium beam. (b) The intermediate milling step is accomplished with a neon beam. (c) The final milling is done with the helium ion beam. (d) The final gap sizes were measured to be as small as 13 nm.

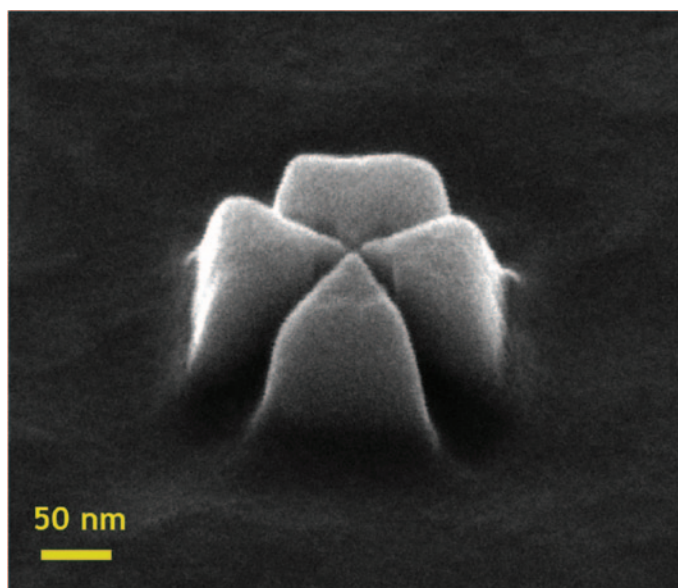


Figure 4: The final structure can be imaged with the same helium beam.

well suited to work in tandem for some demanding fabrication challenges. For example, the preparation of TEM of lamella first requires the bulk removal of material, which is best suited for the gallium beam. Subsequent steps with neon or helium can further remove material or image with fewer vacancies per incident ion and no residual gallium.

This same trend has been exploited in the fabrication of plasmonic devices where nanometer precision is essential and residual gallium is unacceptable. Figure 3a shows a gold film on glass substrate that was patterned with the gallium beam

to remove a square annular region and create a single isolated mesa of gold. The residual gallium was implanted into the glass, but the mesa itself should be free of gallium. Subsequently, a GFIS neon beam with a probe size of about 2 nm and a beam current of about 5 pA was used to mill away along the outer diagonals of the mesa (Figure 3b). Finally, a helium beam with a probe size of <1 nm and a beam current of about 1 pA was used to mill the final cross pattern into the center of the mesa (Figure 3c). In its completed shape, the mesa is split into four symmetric wedges with gaps as small as 13 nm (Figure 3d). Importantly, there is no residual gallium in these gaps. An additional benefit of using the helium beam is that it can also be used for imaging the final structure with minimal damage. The final image (Figure 4) was produced with the same focused helium ion beam used to produce the final steps.

Conclusion

The family of charged particle microscopes is now diverse and specialized. Their relative merits in different roles can be directly attributed to the varying masses of the charged particles. Employing the lightest particles and the most mature technology, electron beam instruments offer high-resolution imaging of sensitive samples together with the well-established X-ray analysis. With seven-thousand times the mass of the electron, the helium ion provides finer image resolution, as well as nanometer-scale sputtering and beam-assisted chemistry. The neon beam, with five times the mass of helium, offers a significantly higher sputter rate and a shallower sample interaction. Neon holds the promise of nanoscale SIMS analysis and extremely sensitive ion beam lithography. Moreover, the most venerable ion beam, gallium, is well established for the high rate of milling available for bulk material removal. Together, the four charged particle beams considered here can provide high-resolution imaging, analysis, and fabrication at the nanoscale. The masses of the respective particles span five orders of magnitude; the disparity in their masses is the basis for their unique capabilities.

Acknowledgments

The author would like to thank the following persons who operated the instruments used for the nanofabrication and imaging of these samples: David Ferranti, Jeff Marshman, and Doug Wei. The following persons provided helpful discussions and review: Charles Lyman, Bipin Singh, and Larry Scipioni.


References

- [1] R Hill, JA Notte, and L Scipioni, "Scanning Helium Ion Microscopy" in *Advances in Imaging and Electron Physics*, ed. PW Hawkes, Academic Press, Boston, 2012.
- [2] F Rahman et al., *Scanning* 33 (2011) 1–6.
- [3] JE Barth and P Kruit, *Optik* 101(3) (1996) 101–09.
- [4] Casino Simulation Software, Version 3.2 (<http://www.gel.usherbrooke.ca/casino/>).
- [5] JF Zeigler, JP Biersack, and U Littmark, *The Stopping and Range of Ions in Matter* (Vol. 1), Pergamon Press, New York, 1985. (The software is freely available at www.srim.org).
- [6] JI Goldstein et al., *Scanning Electron Microscopy and X Ray Microanalysis* (3rd ed.), Springer, New York, 2003.

- [7] R Livengood et al., *J Vac Sci Technol B* 27(6) (2009) 3244–49.
- [8] WJ Arora et al., *J Vac Sci Technol B* 25(6) (2007) 2184–87.
- [9] R Ramachandra, B Griffin, and D Joy, *Ultramicroscopy* 109(6) (2009) 748–57.
- [10] V Castaldo, CW Hagen, and P Kruit, *Ultramicroscopy* 111 (2011) 982–84.
- [11] L Reimer, *Scanning Electron Microscopy: Physics of Image Formation and Microanalysis*, Springer, New York, 1998.
- [12] DC Joy, *Microsc Microanal* 17(4) (2011) 643–49.
- [13] JW Rabalais, *Principles and Applications of Ion Scattering Spectroscopy*, Hoboken, John Wiley and Sons, 2003.
- [14] S Sijbrandij et al., *J Vac Sci Technol B* 28(1) (2010) 73–77.
- [15] A Benninghoven et al., *Secondary Ion Mass Spectroscopy*, John Wiley and Sons, New York, 1987.
- [16] B Cord et al., *J Vac Sci Technol B* 27 (2009) 2616–21.
- [17] V Sidorkin et al., *J Vac Sci Technol B* 27(4) (2009) L18–L20.
- [18] D Winston et al., *Nano Letters* 11 (2011) 4343–47.
- [19] SA Boden et al., *Microelectronic Engineering* 88(8) (2011) 2452–55.
- [20] Livengood et al., *Nucl Instr and Meth A* 645(1) (2011) 136–40.


MT

Minus K[®] Technology's Negative-Stiffness vibration isolators have been selected for ground testing of the James Webb Space Telescope (JWST).



Why have over 2,000 scientists in 35 countries selected Minus K[®] vibration isolators?

Our **Negative Stiffness** systems deliver 10x to 100x better performance than air systems and even better than active systems



Without Minus K[®] With Minus K[®]

The best performance and the lowest price. That's hard to beat!

minus k[®] TECHNOLOGY

460 S. Hindry Ave., Unit C, Inglewood, CA 90301
Tel: 310-348-9656 Fax: 310-348-9638
sales@minusk.com • www.minusk.com

Mention code MT1209 to get a 5% discount on our standard bench top or SM models

ONLY ONE COMPANY SETS THE GOLD STANDARD IN SAMPLE PREPARATION



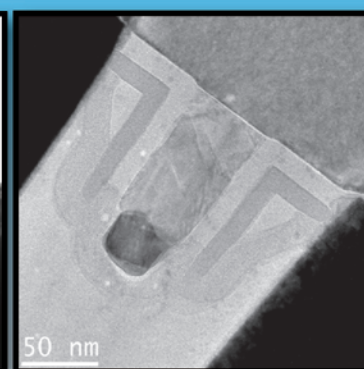
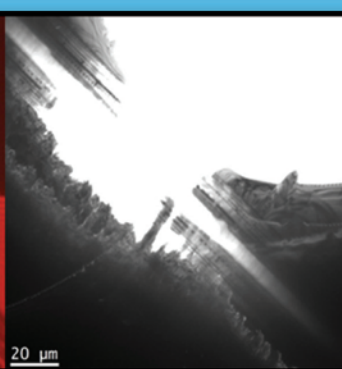
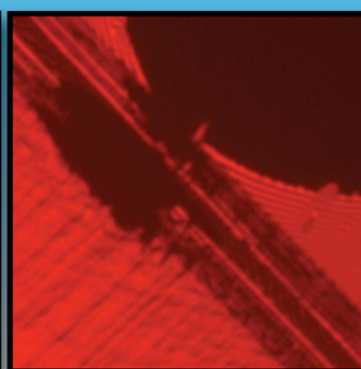
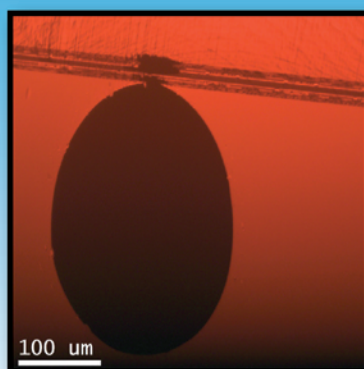
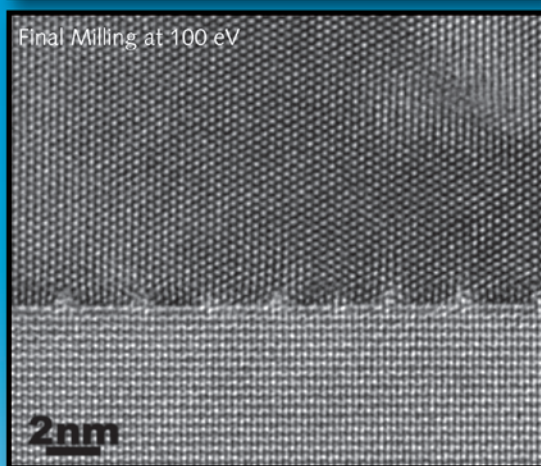
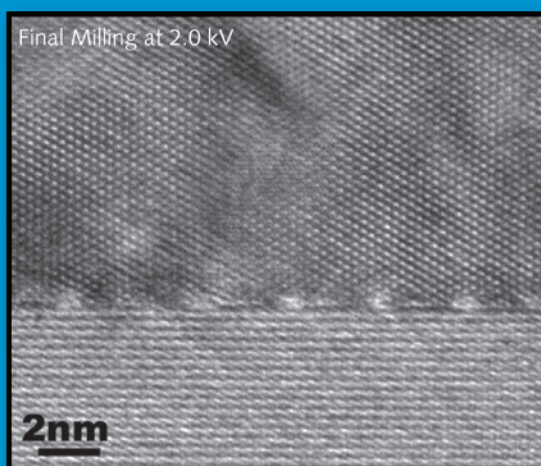
Bench Top Turbo[®] delivers breakthrough carbon evaporation and metal sputtering sample prep in a compact, high-vacuum, fully automatic system.

DENTON VACUUM
BARRIERS BECOME BREAKTHROUGHS

Visit our new website
www.dentonvacuum.com/mt

The Ion Mill You Know: Reborn

Low energy ion guns Cold stage Touch screen Automation and recipes
Live viewing and saving images in Gatan DigitalMicrograph®



Top images: Benefits of low voltage operation: ZnO on Sapphire. Images courtesy of P. Vennégués - CRHEA-CNRS, France.
Bottom images: Series of optical images from Gatan Precision Ion Polishing System II (PIPSTMII) viewing camera and low and high magnification TEM images.



ANALYTICAL TEM
DIGITAL IMAGING
SPECIMEN PREPARATION
TEM SPECIMEN HOLDERS
SEM PRODUCTS
SOFTWARE

PIPS II
Precision Ion Polishing System II